



# Spectroscopic noble gas stack monitor with continuous unattended operation and analysis

James K. Zickefoose<sup>1</sup> · Jonathan L. Burnett<sup>2</sup> · Henrik Persson<sup>1</sup> · Bob Huckins<sup>1</sup> · Troy Anderson<sup>1</sup> · Wilhelm Mueller<sup>1</sup> · Babatunde Oginni<sup>1</sup> · Todd Jokerst<sup>1</sup> · Frazier Bronson<sup>1</sup>

Received: 17 April 2018  
© Akadémiai Kiadó, Budapest, Hungary 2018

## Abstract

A spectroscopic stack monitoring system for the measurement of noble gasses discharged from medical isotope production facility and nuclear power plant stacks has been designed and a prototype constructed. The prototype is based on a Marinelli beaker style HPGe measurement operating in a continuous acquisition mode. Continuous acquisition is accomplished with novel software and hardware which allows for unattended acquisition, analysis, and storage of data over multiple workflow definitions. As a direct result of the multiple averaging times and the use of the transistor reset preamplifier, the dynamic range of the system covers nearly 8 orders of magnitude.

**Keywords** Spectroscopic stack monitoring ·  $^{133}\text{Xe}$  · Noble gas · Continuous analysis · Unattended operation

## Introduction

The release of noble gasses such as  $^{133}\text{Xe}$  through stacks of Nuclear Power Plants (NPPs) and Medical Isotope Production facilities (MIPs) represents a significant source of background to any environmental radioxenon test facility. While both NPPs and MIPs release xenon isotopes to the environment, MIPs do so with a radioxenon isotopic ratio very similar to that of other xenon signals of interest, e.g. nuclear weapons testing [1]. It also has been found that the MIP contribution to the global radioxenon background is significant and that changes in MIP production levels directly affect the global background concentration [2]. Since extremely sensitive environmental radioxenon monitors exist for applications such as nuclear weapons testing monitoring [3], the radioxenon contribution from MIPs and other facilities prove troublesome for the low level measurements.

Typical monitoring installations in nuclear power plants utilize plastic scintillators to monitor beta particles from xenon or krypton decay. While some of these systems have been adapted to measure over a wide range [4], this type of system provides no isotopic information and serves only as a gross measurement technique. Without isotopic information many assumptions must be made to apply this information as a background correction to any low level environmental radioxenon measurements. These assumptions may then reduce the sensitivity of those environmental measurements. Other stack monitors utilize NaI [5, 6] which has the advantage of spectroscopic information, where in principle isotopic information could be extracted. However, the energy resolution of NaI is not sharp enough to separate the peaks of the complicated spectra often observed in noble gas monitoring. In this case the desired isotope identification and quantification is not realized. Finally, there have been a number of radioxenon stack monitors utilizing HPGe detectors and either small sample chambers [7] or xenon holdup in charcoal filters [8]. While HPGe does in fact offer the necessary resolution to properly identify and quantify the isotopes of interest, monitoring of MIP stacks requires the system offer a large dynamic range. Stack concentrations at MIP stacks have been found in the range of  $10^7 \text{ Bq m}^{-3}$  [9] and depending on the time after target irradiation and delay times, that

✉ James K. Zickefoose  
jzickefoose@mirion.com

<sup>1</sup> Miiron Technologies (Canberra) Inc., 800 Research Parkway, Meriden, CT 06450, USA

<sup>2</sup> Pacific Northwest National Laboratory, 902 Battelle Blvd, Richland, WA 99354, USA

number can vary by many orders of magnitude. Therefore, a system with both great sensitivity and ability to measure high concentrations is desired, and in general systems utilizing small sample chambers will not supply the necessary sensitivity. Furthermore, holdup of xenon in charcoal cartridges can be complicated by environmental factors, and consequently the uncertainty associated with the measured concentration may suffer.

## System design

The system described in this paper is based on a Marinelli beaker style measurement, where gas flows through the measurement chamber. The measurement chamber is monitored by a Standard Electrode Germanium detector (SEGe) with approximately 30% relative efficiency. The detector was characterized with In Situ Object Counting System (ISOCS) [10] to allow for efficiency corrections and nuclide identification. The detector is coupled to a Transistor Reset Preamplifier (TRP) which offers a large dynamic range when the proper digital shaping parameters are used. The preamp signals are fed into a Lynx<sup>®</sup> Multi Channel Analyzer (MCA) which utilizes digital signal processing and offers an excellent live time correction. Continuous analysis is accomplished with the Mirion Data Analyst (DA), which is a platform independent analysis module built on existing Genie 2000 analysis engines. Analysis results are stored on the DA but are also transferred to a host computer and stored in a Microsoft Sequel Server database. Historical data including activities, spectra and system health information can then be viewed using the Horizon software. The host computer, DA, MCA, and other electronics are all contained in an environmental enclosure, see Fig. 1.

The sample chamber is shielded by approximately 10 cm of lead where the inner 2 cm of lead are low background lead. The inside of the shield is lined with copper to remove lead X-rays generated in the shield. The shield top is a “split top” design made for ease of access to the sampler. Both the copper lining and the split top design can be seen in Fig. 1, where many of the sampling components are displayed.

The sampling system consists of stainless steel piping designed to connect directly to existing sample lines. The carbon vane pump draws gas through the sampling lines to a particulate and iodine filter. Once the gas has been filtered it then passes into the Marinelli beaker style measurement geometry, fitted with a pressure transducer for pressure corrections. The gas then passes through a mass flow controller, through the pump, and then back out to the stack.

## Theory

ISOCS is a method for characterizing the efficiency of gamma detectors. The process starts with a series of well-defined measurements with small-uncertainty multi-line reference sources. The series of measurements are then used to tune a Monte Carlo N-Particle Code (MCNP) model of the detector and crystal. Once results for all measurements compare well with the modeled efficiencies the benchmarked MCNP model is then used to determine the vacuum efficiencies for the detector over a wide variety of energies between 10 and 7000 keV in a 500 m sphere surrounding the detector. Those efficiencies are then used to generate attenuation corrected efficiencies for geometries of interest. This method was utilized in determining the efficiency of the system over a wide range of energies.

Traditional RC preamps rely on the RC circuit to discharge after each event before the next event is processed. This discharge time is dependent on the RC components used in the circuit, which also play a role in the resolution of the detector [11]. When count rates reach high levels the RC preamp will not be able to discharge completely and will not allow any signal processing at all. Unfortunately, when the RC preamp is tuned for high count rates the resolution suffers. TRPs on the other hand do not rely on RC feedback to discharge the circuit. In this case the circuit is forced back to its baseline by a transistor reset. In this way, even at extremely high count rates the circuit never paralyzes and spectra can continue to be collected [12].

The Data Analyst is a device that runs the MCA in Multi Spectral Scaling (MSS) mode, where spectra are continuously acquired in 1 s intervals. These one second intervals are then summed together to form spectra with desired acquisition intervals. Since the DA is continuously acquiring and storing 1 s spectra for analysis, it has the ability to perform parallel analyses on one data stream. For instance, the DA may acquire 1, 10 min, 1, and 4 h analysis intervals on a single data stream simultaneously. The analysis parameters for these separate “workflows” may be set independently such that separate analysis algorithms, nuclide libraries, or even efficiency calibrations may be utilized for each workflow. In this way, using both short and long averaging times allows for both swift reaction times for dynamic conditions as well as low Minimum Detectable Concentrations (MDCs) for stable conditions. The DA is also designed to run completely unattended. It will automatically perform the analysis sequence at the end of each respective “workflow” and store the results both locally on the device and in a remote database.

The standard Currie formalism [13] was used to calculate the MDC where:

**Fig. 1** The environmental enclosure, left, and sampling skid, right. The enclosure houses the electronics and central computer while the detector, sampling chamber, sampling components, and the shield are located on the sampling skid



$$\text{MDC} = \frac{k^2 + 2k\sqrt{2\dot{B}T}}{\epsilon\gamma T} \quad (1)$$

where  $k$  is the confidence interval,  $B$  is the background rate in the ROI,  $T$  is the measurement time,  $\epsilon$  is the efficiency at the ROI energy, and  $\gamma$  is the yield of the gamma ray in question.

## Experimental

The energy and shape calibration was carried out using  $^{241}\text{Am}$ ,  $^{152}\text{Eu}$ , and  $^{228}\text{Th}$  sources giving a range in energy from 59.5 keV up to 2614 keV. Efficiency calibration was performed using the ISOCS methodology and verified with calibrated gas measurements of  $^{85}\text{Kr}$  and  $^{133}\text{Xe}$  which confirm the efficiency at 514 and 81 keV respectively. Verification measurements utilized Eckert and Zeigler glass sphere calibration sources which were injected into the system using calibrated gas syringes. Before injection a vacuum was drawn on the sampler, the gas was then injected into the sampler through a rubber stopper. The atmosphere was allowed to fill the chamber through a vent needle, mixing the gas in the process. Repeated acquisitions were carried out during the process and the spectra were collected by the system, including profiles during

injection, during a steady state measurement, and then during the venting process.

The shielding effectiveness of the system was tested in a 100 nSv  $\text{h}^{-1}$  ambient field where the measurement chamber had previously been vented thoroughly. The test was run overnight and spectra were acquired in 1 h intervals and then summed together to determine the average count rate for a number of relevant ROIs.

Energy resolution is an important parameter that is a measure of how neighboring peaks may be resolved from one another. A better energy resolution will also reduce the minimum detectable concentration because a narrower ROI may be used for analysis. The performance of the system at high count rates was both optimized and verified. Optimization was conducted by cycling through the MCA shaping parameters, rise time and flat top, while determining the effect on energy resolution and dead time. A  $^{152}\text{Eu}$  source was used during optimization and the resolution at 121 and 1408 keV was monitored.

The live time correction for a signal chain corrects the acquisition period for time when the detector could not register an event, i.e. the detector is dead. This happens every time the system is processing an event. The more signals a signal chain is processing the greater the amount of time the system is dead. At very high count rates this dead time can be a large percentage, e.g. 99%, of the real time during an acquisition. Therefore, it is important that the dead time is correctly calculated by a system experiencing high count rates or the reported activity may be

systematically wrong by a large margin. Once ideal shaping parameters were chosen, the performance of the live time correction was then tested at the optimal settings. The live time correction was tested by placing a reference  $^{137}\text{Cs}$  source at a fixed location relative to the detector and noting the count rate in the 662 keV peak. A  $^{152}\text{Eu}$  source was then introduced to elevate the count rate. The count rate was elevated further by continuously moving the  $^{152}\text{Eu}$  source closer to the detector while monitoring the count rate in the  $^{137}\text{Cs}$  peak. For a perfect live time correction the count rate in the 662 keV peak should not change outside of counting statistics. The results of the live time correction study determines the maximum allowable count rate for the system, defined as the point where the live time correction deviates by more than 5% from the true rate.

During the efficiency verification measurements the total spectrum count rate was noted for  $^{133}\text{Xe}$ . With full spectrum efficiency and the characterized maximum count rate of the system, the maximum measurable concentration of the system can be determined by dividing the maximum allowable count rate by the full spectrum efficiency.

The efficiency verification measurements also served as a means to determine the retention of the system for noble gases. Since the spectra were collected both during the static efficiency measurement and during the venting process, it was possible to determine the time to remove all detectable traces of radionon from the sample chamber. The chamber was vented overnight and spectra were continuously acquired to determine the retention for xenon and krypton.

## Results and discussion

Comparisons of the ISOCS efficiencies to the verification measurements are shown in Fig. 2 where the overlaid verification measurements compare well. The ratio of ISOCS to measured efficiency was found to be 0.99 and 0.97 at 81 keV ( $^{133}\text{Xe}$ ) and 514 keV ( $^{85}\text{Kr}$ ) respectively. Uncertainties in the measured efficiencies stem primarily from uncertainty in the activity concentration of the gas and were found to be 2.3 and 3.2%, at the  $1\sigma$  level, for the 81 keV ( $^{133}\text{Xe}$ ) and 514 keV ( $^{85}\text{Kr}$ ) respectively. During the  $^{133}\text{Xe}$  measurement, the full spectrum efficiency was also determined. The  $^{133}\text{Xe}$  full spectrum efficiency was found to be  $4.2 \pm 0.1 \times 10^{-3}$  cps  $\text{Bq}^{-1}$ ; this value will be used to calculate the maximum measurable concentration once the maximum count rate is determined.

Background rates were measured with a closed shield overnight and the full spectrum background rate was found to be  $2.73 \pm 0.02$  cps. The 81 keV ( $^{133}\text{Xe}$ ) and 514 keV

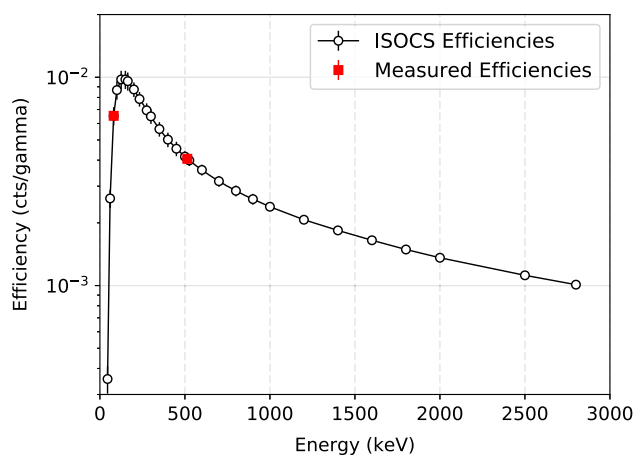


**Fig. 2** Comparison of ISOCS efficiencies for the measurement geometry to verification measurements made with gas standards. The verification energies are 81 keV,  $^{133}\text{Xe}$ , and 514 keV,  $^{85}\text{Kr}$ . Agreement in both cases was within the measurement uncertainty at the  $1\sigma$  level

( $^{85}\text{Kr}$ ) ROIs were found to have  $0.013 \pm 0.02$  and  $0.0096 \pm 0.0008$  cps respectively.

High count rate performance was characterized by first optimizing the digital shaping parameters, rise time and flat top, and then testing the performance over a variety of count rates. Initial testing showed that even small changes in the flat top resulted in large degradation of the energy resolution. Therefore, the flat top was held constant at  $0.8 \mu\text{s}$  while the rise time was varied. Changes in the rise time showed much less effect on the energy resolution, but in general as the rise time was decreased the resolution degraded. Curves for the  $^{152}\text{Eu}$  121 and 1408 keV lines are shown in Fig. 3 where the resolution is generally flat

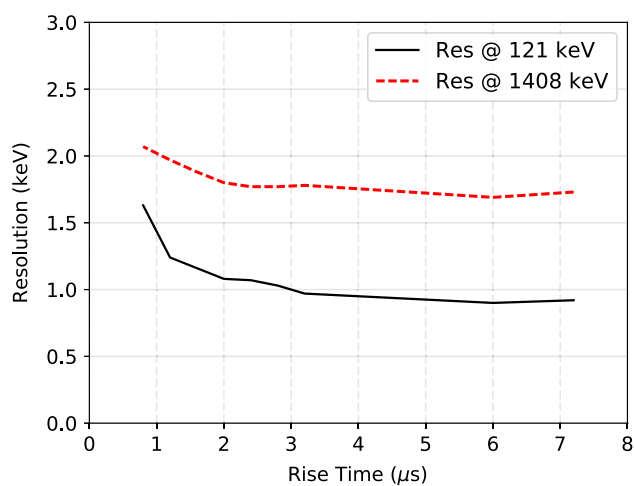


**Fig. 3** Energy resolution as a function of rise time at 121 and 1408 keV for count rates below 1000 cps. In all cases the flat top shaping parameter was held fixed at  $0.8 \mu\text{s}$

between approximately 3 and 7.2  $\mu\text{s}$ , but then increases below 3  $\mu\text{s}$ .

While Fig. 3 shows the behavior at low count rates and low dead times, the same experiment was repeated at very high count rates, 500 kcps, as well. Figure 4 shows the trend of energy resolution as a function of rise time at 500 kcps, where again resolution begins to degrade below approximately 3  $\mu\text{s}$ , but also degrades above 6  $\mu\text{s}$ . The increase in resolution at long shaping times is now likely due to interference of successive pulses in the preamp, while the continued degraded resolution at very short rise time is likely due to only fractions of each pulse being analyzed.

In order to optimize and study the performance of the system at high count rates, the dead time was determined as a function of count rate and rise time. Figure 5 shows the relationship between rise time and dead time for a variety of input count rates. Clearly as the count rate increases the dead time increases for a given rise time, and the dead time increases as the rise time increases for a given count rate. The rise time was optimized to give a low dead time for a given count rate, as found in Fig. 5, while still holding an optimal resolution over all count rates, as found in Figs. 3 and 4. The optimal rise time was chosen to be 2.8  $\mu\text{s}$ , and along with the flat top of 0.8  $\mu\text{s}$ , these values were used for the remainder of the testing.

With the shaping parameters determined, the performance of the system as a whole was now investigated. As previously mentioned, the accuracy of the live time correction is of great importance at high dead times. The accuracy of the Lynx live time correction was tested using the dual source method: one source was held at a fixed position relative to the detector to produce a stable count rate in a reference peak, while another source of high

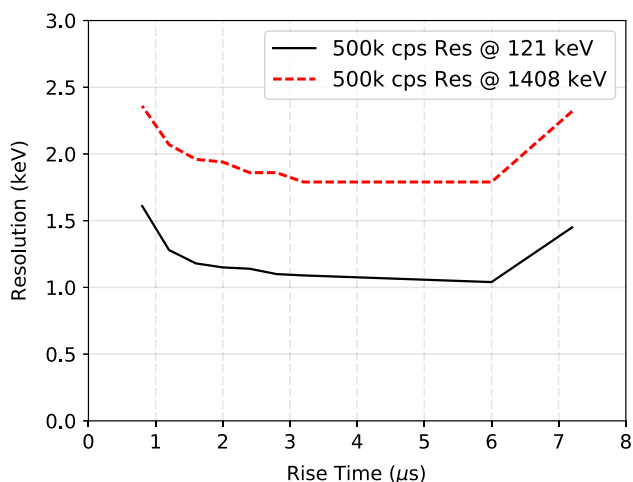


**Fig. 4** Energy resolution as a function of rise time at 121 and 1408 keV for count rates at 500 kcps. In all cases the flat top shaping parameter was held fixed at 0.8  $\mu\text{s}$

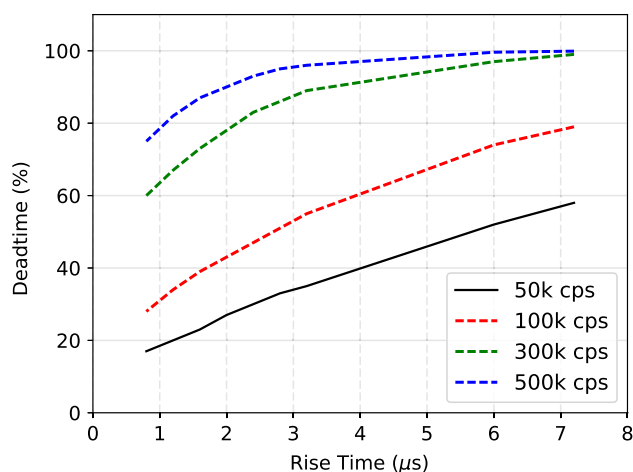


**Fig. 5** Deadtime as a function of rise time parameter for a variety of count rates. Clearly as the rise time increases the deadtime increases for a given count rate

activity and a different nuclide was placed at various distances relative to the detector to vary the total spectrum count rate. The stable source was chosen to be  $^{137}\text{Cs}$  with a peak at 662 keV, while the source that was moved to create various count rates was  $^{152}\text{Eu}$ . To determine the accuracy of the live time correction the count rate in the 662 keV  $^{137}\text{Cs}$  peak was monitored throughout the experiment. Since the source was held at a fixed position relative to the detector, the count rate in that peak should not change. Figure 6 shows the ratio of counts in the 662 keV peak at various dead times relative to that at a low dead time, 2%. The results indicate that the live time correction of the Lynx is accurate within 5% up to 94% dead time, or 510 kcps. Therefore, 500 kcps was used as the upper count rate limit of the system, even though it will continue to function above that rate.

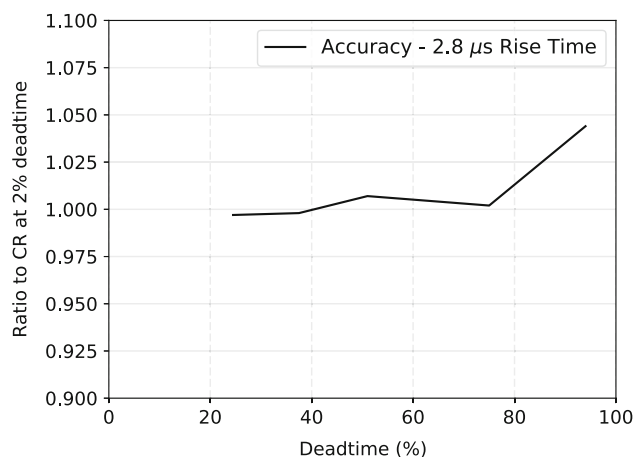


**Fig. 6** Accuracy of the live time correction as a function of count rate using the two source method. There was no significant error in the live time correction up to 75% deadtime and less than 5% error at 94% deadtime

**Table 1** Derived minimum detectable concentrations at the 95% confidence level for various nuclides at various averaging times

Nuclide	MDC (Bq m <sup>-3</sup> )		
	600 s acquisition	3600 s acquisition	14,400 s acquisition
<sup>85</sup> Kr	6.9E+04	2.5E+04	1.2E+04
<sup>85m</sup> Kr	1.9E+02	6.8E+01	3.3E+01
<sup>131m</sup> Xe	7.4E+03	2.7E+03	1.3E+03
<sup>133</sup> Xe	5.7E+02	2.1E+02	1.0E+02
<sup>133m</sup> Xe	1.6E+03	5.7E+02	2.7E+02
<sup>135</sup> Xe	1.9E+02	6.8E+01	3.2E+01
<sup>135m</sup> Xe	2.5E+02	8.3E+01	3.8E+01

The performance of the system was also determined in terms of maximum measurable concentration, Minimum Detectable Concentration (MDC), and retention for noble gasses. With the maximum measurable count rate determined as 500 kcps and the full spectrum efficiency,  $4.2 \pm 0.1 \times 10^{-3}$  cps Bq<sup>-1</sup>, determined from a <sup>133</sup>Xe measurement, the maximum measurable concentration of <sup>133</sup>Xe can now be determined. The maximum measurable concentration was found to be  $6.4 \times 10^9$  Bq m<sup>-3</sup>, and if the stack flow rate is taken to be 90,000 m<sup>3</sup> h<sup>-1</sup>, the maximum measurable release rate is found to be  $5.7 \times 10^{14}$  Bq h<sup>-1</sup>. The maximum measurable concentration and release rate are both in reference to <sup>133</sup>Xe; other nuclides will vary depending on line energies and intensities.

Environmental background measurements conducted with a closed shield showed the total spectrum count rate in a 100 nSv h<sup>-1</sup> ambient background was 0.0127 for the 81 keV ROI, <sup>133</sup>Xe. Using the Currie formalism with  $k = 1.96$ , at the 95% confidence level, and the ROI background rates determined during the environmental background measurement the MDC values for a number of nuclides were found. These MDC values for a variety of count rates are displayed in Table 1, where the ability of the system to maintain separate workflows in parallel to set various averaging intervals may be taken advantage of to retain reasonable response time, such as 10 min, and extend another averaging interval, to 4 h for example, to attain a low MDC.

During the verification measurements with <sup>133</sup>Xe and <sup>85</sup>Kr the stainless steel sampler was tested for any memory effects of noble gas retention. In this case the peak count rate for each nuclide was monitored both during the injection of the calibration gas and then during the venting process. In the case of either nuclide it was found that the peak count rate rapidly decreased during the venting process and stabilized at the typical background count rates within 2 h.

Finally, during the <sup>85</sup>Kr measurements the energy resolution at 514 keV was found to be approximately 1.3 keV, which allows for separation of the 514 keV peak from any

511 keV annihilation peak that may be present during operation.

## Conclusions

A spectroscopic noble gas stack monitoring system has been developed and tested. The use of the Data Analyst alongside the Lynx MCA allows for continuous and unattended operation where Genie 2000 analysis algorithms are executed and the results stored continuously. The availability of multiple workflows being set in parallel allows for both fast reaction times as well as excellent sensitivity. Performance testing of the system shows that the range of the system for <sup>133</sup>Xe is approximately 100 to  $6.4 \times 10^9$  Bq m<sup>-3</sup>, where the high end is attained by the use of a transistor reset preamplifier. While the system was designed for characterization of the source term from facility stacks, the range of the system also lends itself to routine stack monitoring at those same facilities. Future work includes commissioning of systems at MIPs, research facilities, and NPPs, where the results may be used to estimate the contribution of each facility to the global radionuclide background.

## References

1. Saey P, Bowyer T, Ringborn A (2010) Isotopic noble gas signatures released from medical isotope production facilities—simulations and measurements. *Appl Radiat Isot* 68:1846–1854
2. Hoffman I, Ungar K, Bean M, Yi J, Servranckx R, Zaganescu C, Ek N, Blanchard X, Petit GL, Brachet G, Achim P, Taffary T (2009) Changes in radionuclide observations in Canada and Europe during medical isotope production facility shut down in 2008. *J Radioanal Nucl Chem* 282(3):767–772
3. Ringborn A, Larson T, Axelsson A, Elmgren K, Johansson C (2003) SAUNA—a system for automatic sampling, processing, and analysis of radioactive xenon. *Nucl Instrum Methods Phys Res A* 508(3):542–553
4. Takasaki K, Kobayashi H, Suzuki H, Ushigome S (2010) Wide-range krypton gas monitor using a plastic scintillation detector

- operated in current mode with a gate circuit. *J Nucl Sci Technol* 47(3):255–261
5. Lee B, Jester W, Olynyk J (1992) On-line radioiodine measurement using hot cell effluent gases of a radiopharmaceutical production facility. *Nucl Technol* 97(1):63–70
  6. Jabs R, Jester W (1976) The development of an environmental monitoring system for the continuous detection of low-level radioactive gases. *Nucl Technol* 30(1):24–32
  7. Xie F, He X, Jiang W, Zhang X, Shi Q, Wu S, Liu L, Zhang C, Chen L (2014) Development of a radioxenon measurement system and its application in monitoring Fukushima nuclear accident. *Radiat Phys Chem* 97:85–89
  8. Deconninck B, Lellis CD (2013) High resolution monitoring system for IRE stack releases. *J Environ Radioact* 125:61–68
  9. Saey P, Ringbom A, Bowyer T, Zahringer M, Auer M, Faanhof A, Labuschagne C, Al-Rashidi M, Tippawan U, Verboomen B (2013) Worldwide measurements of radioxenon background near isotope production facilities, a nuclear power plant and at remote sites: the “Eu/JA-II” project. *J Radioanal Nucl Chem* 296(2):1133–1142
  10. Venkataraman R, Bronson F, Atrashkevich V, Young BM, Field M (1999) Validation of in situ object counting system (ISOCS) mathematical efficiency calibration software. *Nucl Instrum Methods Phys Res A* 422:450–454
  11. Knoll G (2010) Radiation protection and measurement, 4th edn. Wiley, Hoboken, pp 356–359
  12. Landis D, Cork C, Maddden N, Goulding F (1982) Transistor reset preamplifier for high count rate high resolution spectroscopy. *IEEE Trans Nucl Sci* 29(1):619–624
  13. Currie L (1968) Limits for qualitative detection and quantitative determination. *Anal Chem* 40:586–593